

Experiment E101- Acoustic Optical Moduel

Robin Hoffmann*, Arik Bürkle[†], Valentin Ertl[‡]

June 10, 2025

Abstract

In this experiment, we characterize the Acoustic Optical Module (AOM), specifically the AOMO 3080-125, by probing it with a laser and measuring the distance of the first and zeroth Bragg maxima and the intensity of those maxima. From this, we calculated a saturation power of $1,32(5)$ W, a quality factor of $0,63(2)$, and the Bragg angle at $f_{RF} = 80$ MHz to be 6 mrad

*robin.hoffmann@student.uibk.ac.at

[†]arik.buerkle@student.uibk.ac.at

[‡]valentin.ertl@student.uibk.ac.at

Contents

1	Introduction	1
2	Theory	2
2.1	Bragg reflection	2
2.2	Function of a AOM	3
2.3	Properties of an AOM	4
2.4	Converting the voltage to power.	4
3	Experiment setup and execution	5
3.1	Experimental setup and functionality	5
3.2	Experimental procedure	9
3.2.1	Measurement of the electronic components and the optimal Bragg angle	9
3.2.2	Measurement of intensity dependence and determination of saturation power	9
3.2.3	Measurement of frequency dependence and determination of the quality factor	9
3.2.4	Measurement of angular dependence and comparison of the quality factor	9
3.2.5	Measurement of the angular dependence of the maximum diffraction efficiency	9
4	Ergebnisse	10
4.1	Measurement of the Bragg angle	10
4.2	Measurement of intensity dependence and determination of saturation power.	10
4.3	Measurement of frequency dependence and determination of the quality factor	11
4.4	Measurement of angular dependence and comparison of the quality factor	13
4.5	Measurement of the angular dependence of the maximum diffraction efficiency	14
5	Disscution	15

1 Introduction

In the world of optics, acousto-optic modulators play a crucial role in the precise control and manipulation of light. These fascinating devices use the acousto-optic effect, in which sound waves modulate the optical properties of a material (in this experiment crystal) to change the frequency, phase or intensity of light waves. A fundamental theory underlying the operation of AOMs is Bragg diffraction, based on the principle of constructive interference of scattered light. Bragg diffraction, named after physicists Sir William Henry Bragg and his son Sir William Lawrence Bragg, describes the phase relationship between incident and scattered light waves on a periodic lattice. In the context of an AOM, Bragg diffraction is applied to determine the conditions under which the interaction between light and sound leads to constructive interference, resulting in efficient modulation of the light signal [1][2]. The fundamental formula of the Bragg condition is: $n\lambda = 2\Lambda\sin(\theta_i)$. Where Λ represents the periodicity of the lattice, θ_i denotes the angle between the incident light wave and the lattice (= angle of incidence), n is the diffraction order, and λ is the wavelength of the light. In this experiment we used a helium-neon (He-Ne) laser with a wavelength of 632,8 nm [1].

The following report begins by explaining the theory behind how an AOM works in more detail. So that all necessary aspects for the theoretical understanding of the experiment are clarified. The experimental setup and the execution are then illustrated and explained step by step. The recorded data is then analyzed and the results presented. Finally, the results are discussed and possible conclusions are drawn.

2 Theory

This section discusses the function of Bragg reflection, how an acousto-optic modulator (AOM) forms a lattice structure, and how the resulting lattice structure influences the Bragg maxima.

2.1 Bragg reflection

An electromagnetic wave with a certain wavelength λ is only reflected by a crystal if it hits the crystal at very specific angles (Bragg angles). This phenomenon is described by the Bragg equation

$$n\lambda = 2\Lambda \sin(\theta_i) \quad (1)$$

As mentioned earlier in the introduction, the Bragg equation describes the conditions under which constructive interference, and thus reflection from a crystal, occurs. It establishes a relationship between the Bragg angles θ_i , at which constructive interference occurs, the lattice plane spacing of the crystal Λ , the diffraction order n , and the wavelength λ of the incident radiation [3]. The derivation of the Bragg equation is outlined in the following figure, where our Λ corresponds to d .

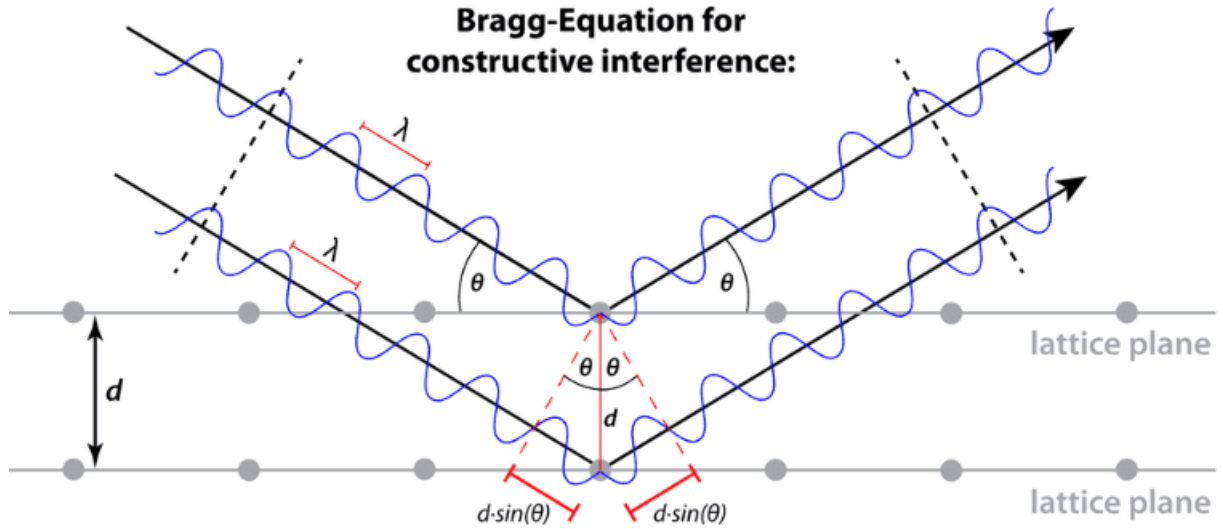


Figure 1: Beam path of Bragg reflection at constructive interference. [4]

It is precisely this Bragg reflection that the AOM makes use of and is therefore integrated into its mode of operation.

2.2 Function of a AOM

In an AOM, optical light gets refracted by an acoustic wave, as shown in Fig. 2. There are two ways to interpret this effect. In quantum mechanics, the photons of the laser beam interact with the phonons of the crystal. According to the conservation of momentum, the photon gets redirected with the new momentum (Eq. 2):

$$p_{out} = p_{in} + p_{RF} \quad (2)$$

Not every photon interacts with a phonon, meaning that some of the light passes through the crystal without interacting.

A simpler way to view this system is to take a classical approach. Here, the crystal gets deformed

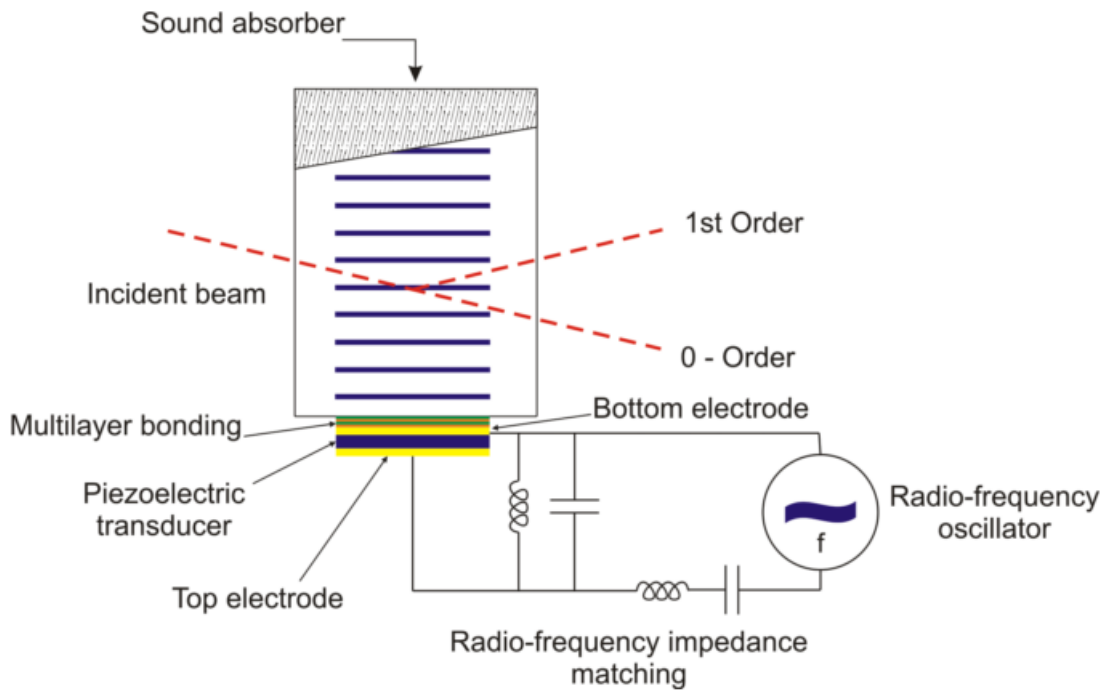


Figure 2: Schematics of an AOM with indicated acoustic waves inside the crystal, forming regions of different densities and creating a lattice structure inside the crystal from where the light can be reflected [5].

by the acoustic wave, forming sections with a higher refractive index and some areas with a lower refractive index. This periodicity corresponds to the wavelength of the acoustic wave, giving us a lattice structure with a lattice spacing Λ . The connection between lattice spacing and the radio frequency (f_{RF}) is given by Eq. 3:

$$\Lambda = \frac{f_{RF}}{V_s} \quad (3)$$

Here, V_s represents the speed of sound inside the crystal. This means that a quasi-crystal structure is formed, and from the Bragg condition (Eq. 1), we obtain the angle for the first-order maximum.

2.3 Properties of an AOM

An AOM has a lot of characteristic properties depending on the light, the crystal used, and the layout of the crystal, to name a few. These characteristics are often provided by the manufacturer, but it is also possible to measure them.

One of those properties is the insertion loss IL , describing the amount of power lost inside the crystal. This can be described by Equation 4, where P_{in} describes the ingoing power and P_{out} the outgoing power.

$$IL = 1 - \frac{P_{out}}{P_{in}} \quad (4)$$

The most important one is the dispersion efficiency ϵ . It describes the amount of power that gets dispersed in the crystal, which is the power of the first maximum (Eq. 5):

$$\epsilon = \frac{P_1}{P_{out}} \quad (5)$$

This efficiency depends on the power of the RF P_{RF} and also on the variation from the Bragg angle δ of the laser compared to the crystal. When we assume that the crystal is at the Bragg angle θ_B , the efficiency only depends on the power of the RF, as shown in Eq. 6.

$$\epsilon \propto \sin^2 \left(\frac{\pi}{2} \sqrt{\frac{P_{RF}}{P_{sat}}} \right) \quad (6)$$

Here, P_{sat} is the saturation power. When we hold the power constant, the efficiency only depends on the deviation of the Bragg angle, $\Delta = \delta/\theta_B$.

$$\epsilon \propto \text{sinc}^2 \left(\frac{Q}{4} \Delta \right) \quad (7)$$

This efficiency mainly depends on the quality factor Q , which describes the relative interaction length in the crystal. If we vary the frequency, the angle gets offset by a small amount. We can define the relative variation with $F = f/f_0$. From this, the dependence of the efficiency is dependent on the frequency.

$$\epsilon \propto \text{sinc}^2 \left(\frac{Q}{4} F(1 - F) \right) \quad (8)$$

2.4 Converting the voltage to power.

In this experiment, we used a function generator to generate the acoustic wave, where the power of this wave is related to the peak-to-peak voltage of the electrical signal. This electrical signal is then amplified by an amplifier, providing the wave with additional power. In our experiment, the voltage of the amplifier was held constant, ensuring consistent amplification. From the data provided by the producers, we gathered that the amplifier adds around 33,4(2)dBm to our electrical signal. This provides a relationship for the power of the acoustic wave P_{RF} to the input

voltage U_{in} as shown in Eq. 9, where U_0 is the reference voltage of 632 mV.

$$P_{RF} = \left(\frac{U_{in}}{U_0} \right)^2 \cdot 10^{\frac{33,4(2)}{10}} mW \quad (9)$$

3 Experiment setup and execution

This section explains the functionality as well as the structure and implementation of the experiment.

3.1 Experimental setup and functionality

The experiment is set up as shown in figure 4. The He-Ne laser (1.) is guided to the AOM (3.) via various mirrors (2.) and focusing lenses (5.). This is where the Bragg diffraction takes place. The light of the plane wave with the corresponding angle of incidence is split into the different diffraction orders at the lattice structure of the crystal. The amplifier (4.) controls the RF power and thus the amplitudes of the sound waves that pass through the crystal. After the laser beam has passed the AOM (3.) and been split into the various diffraction orders, these are redirected via mirrors (2.) and a focusing lens (5.) to the power meter (6.). The power meter can then be used to measure the intensity of the individual diffraction orders. The most important dimensions in Figure 4 are:

- from the AOM output (3.) to the first mirror (2.): 11.3 cm
- From the first mirror (2.) to the second mirror (2.) to the left: 15.4 cm
- from the second mirror (2.) to the power meter (6.): 25.6 cm
- from the second mirror (2.) to the target (wall), which is not shown in figure 4: 138,5 cm

All dimensional errors were estimated at 2 mm. Which comes from the uncertainties finding the center of the mirror and the scaling of our ruler.

Figure 3 depicts the setup of the experiment in a schematic manner once again. However, in our case, the laser beam is redirected more frequently via mirrors than shown in this figure. Nevertheless, this does not affect the data acquisition and analysis.

As evident in Figure 3, besides recording the powers of the different diffraction orders (in our experiment, only 0th and 1st order) using the power meter, one can also measure the angular separation θ between the two orders. For this purpose, the two laser beams of the respective orders are projected onto a target (in our case, a wall) with sufficient spacing, and the distance between the light spots of the adjacent diffraction orders is measured. Subsequently, the angular separation can be calculated from this distance.

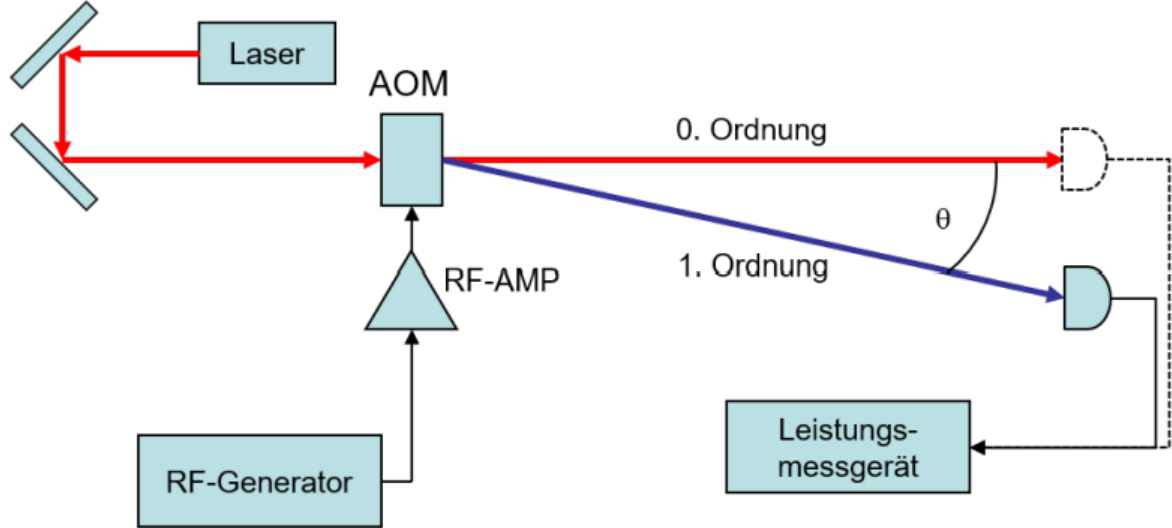


Figure 3: Sketch of the experimental setup. [1]

We would now like to take a closer look at the internal structure of the AOM (3.). The RF input signal is transmitted to a piezoelectric transducer via an electronic matching circuit, which generates acoustic waves in the AOM crystal. These acoustic waves manifest as density changes in the medium, leading to periodic variations in the refractive index. The acoustic waves traverse the crystal and are selectively absorbed at the other end. A laser beam, incident at the proper angle (Bragg condition), is split into multiple diffraction orders. Under optimal coupling and moderate RF power, the 0th and 1st orders are the dominant components. Figure 5 illustrates the internal structure of an AOM.

Furthermore an RF signal generator (7) is used to operate the AOM with variable RF frequencies and powers. This allows us to vary the frequencies and the power at which the amplifier and the AOM are operated in the experiment and thus control the amplitudes of the sound waves. We can therefore increase or decrease the modulation rate of the light beam. The amplifier (8) takes the resulting RF signal and amplifies it by around 33.4(2) dBm. In our experiment, a voltage of 24 volts was applied continuously for the duration of the experiment. Figure 6 below shows the two experimental components.

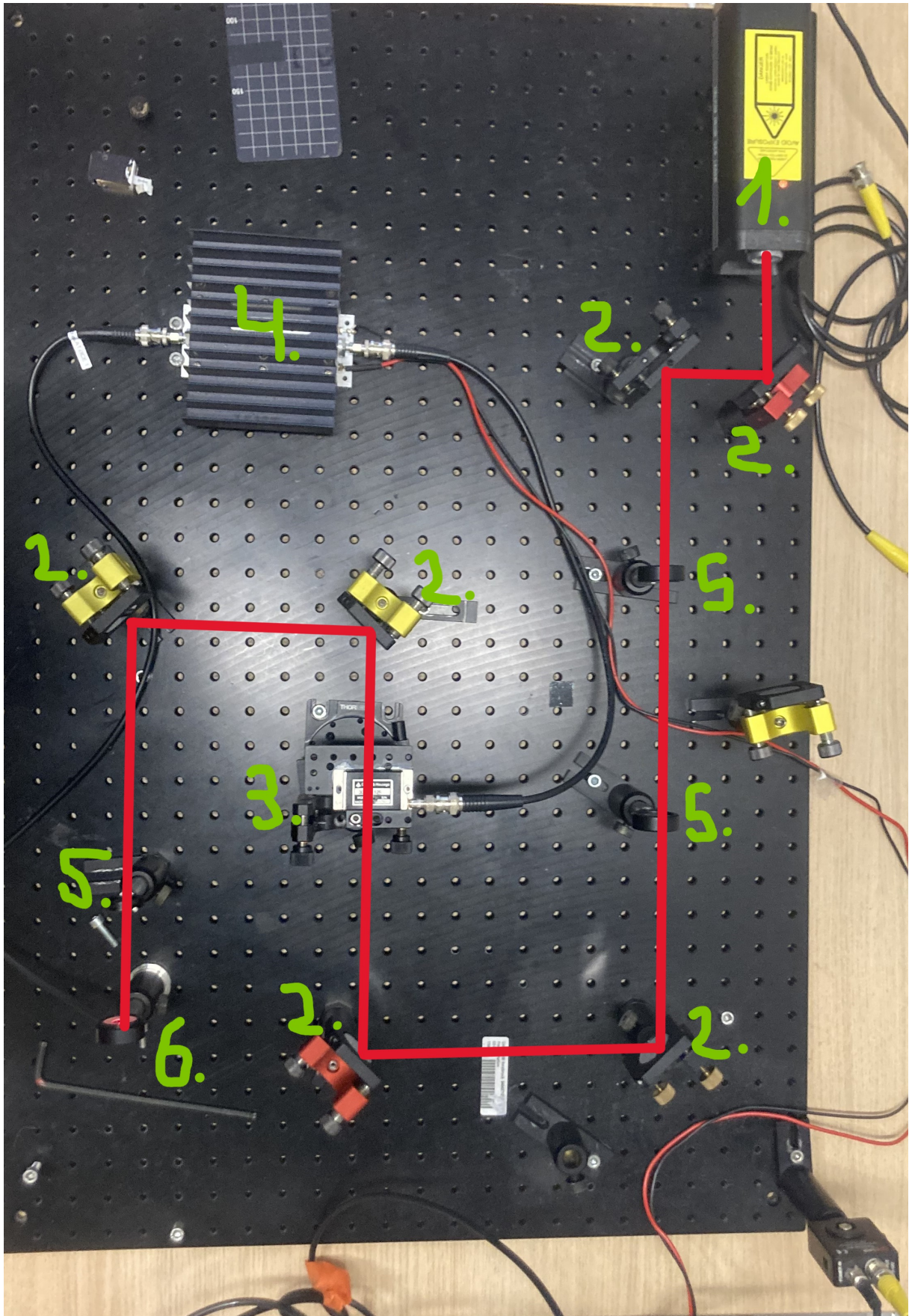


Figure 4: Illustration of the experimental setup. 1. He-Ne laser, 2. mirror, 3. AOM, 4. amplifier, 5. focusing lense, 6. power meter.

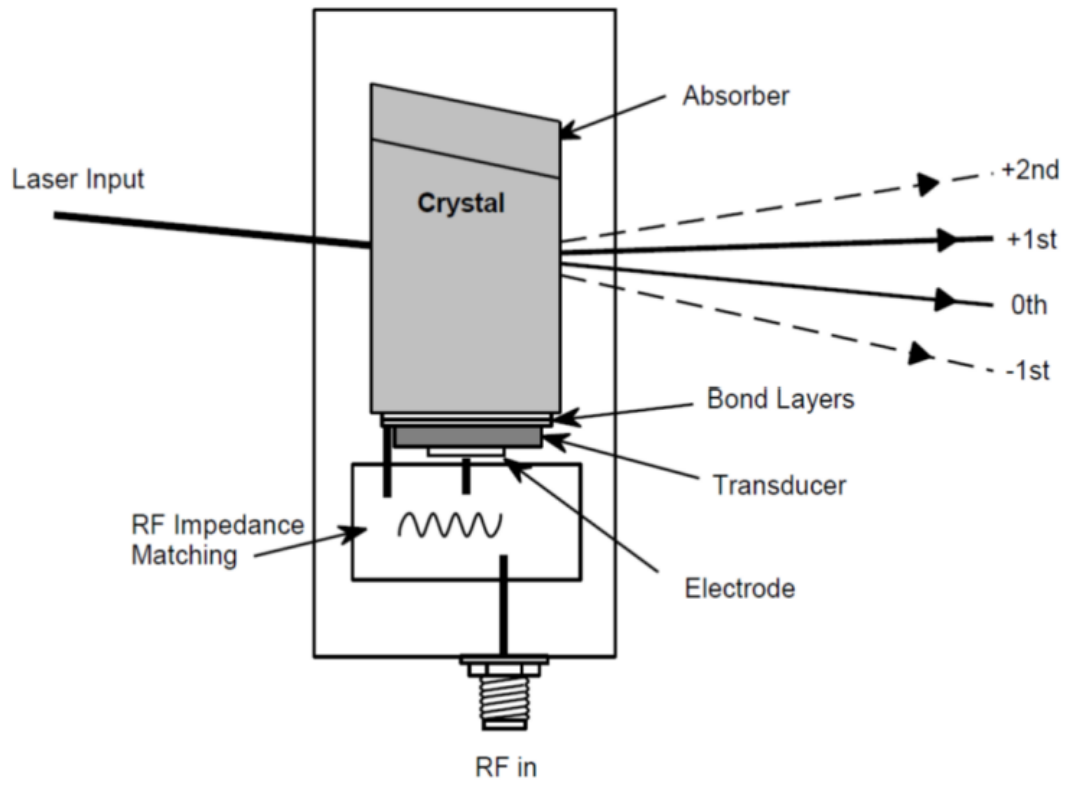


Figure 5: Internal structure of an AOM. [1]

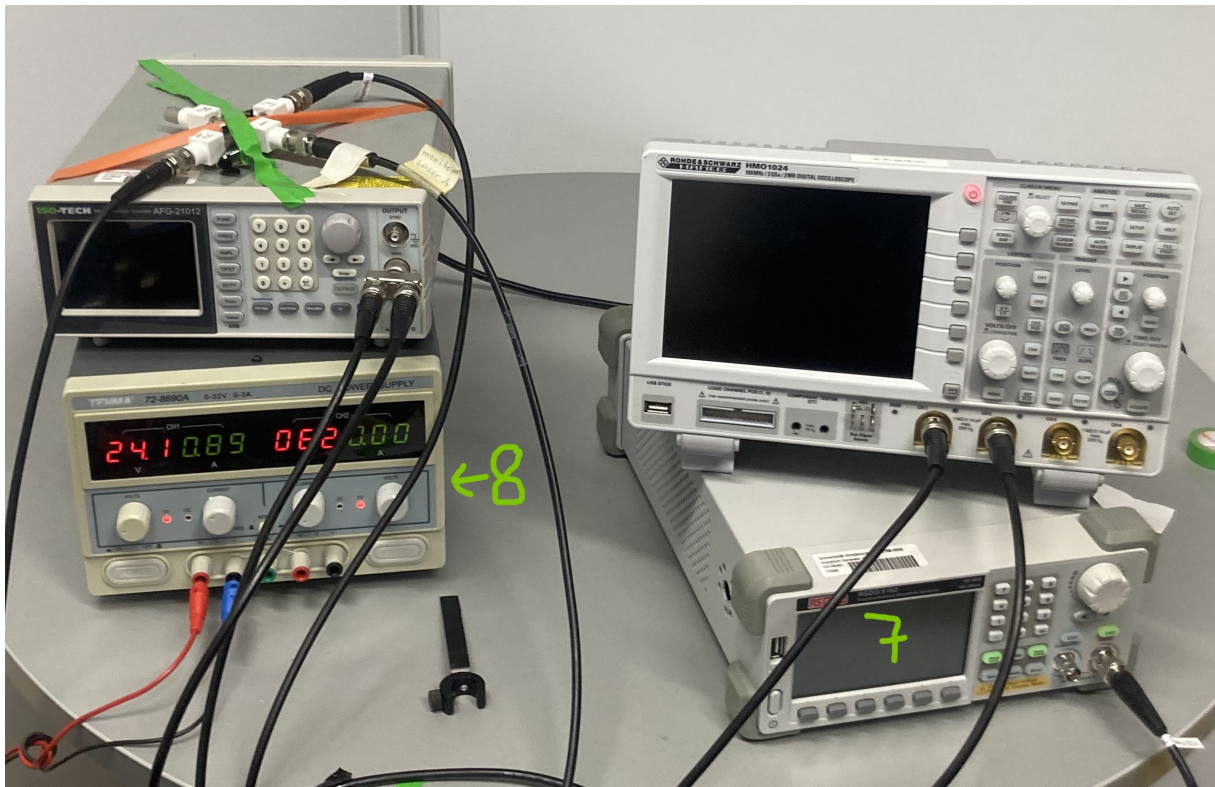


Figure 6: RF signal generator (7) for operating the AOM with different powers or frequencies and amplifier (8) for amplifies the signal.

3.2 Experimental procedure

In this chapter, the methodology and steps undertaken during the experiment are outlined.^[1]

3.2.1 Measurement of the electronic components and the optimal Bragg angle

In the initial measurement, the optimal Bragg angle is to be set and determined. At the beginning we calculate the required values in mVpp for output powers of 0,5 W, 1 W, and 2 W using a provided value table, ensuring they are readily available for subsequent measurements. Subsequently, the AOM is operated at its central RF frequency f_{RF} (80MHz) with a power of 1W. After the initial beam coupling, the angle of the AOM is optimized to maximize the power in the 1st order using the power meter. At a sufficient distance (after redirection through two additional mirrors), the separation between the 0th and 1st orders is measured, from which the optimal Bragg angle for 80MHz is determined and compared with the specifications from the datasheet.

3.2.2 Measurement of intensity dependence and determination of saturation power

Now, the total power is first determined before and after the AOM without the RF power P_{RF} , and then the insertion loss IL is calculated. Subsequently, the RF power is swept from 0 W to 2 W, and the power of the 0th and 1st orders is recorded for each step. Then, the diffraction efficiency ϵ is calculated as a function of power, and the measurement is compared with theory. At the end of this sub task, the saturation power is determined through an appropriate fit.

3.2.3 Measurement of frequency dependence and determination of the quality factor

Prior to this measurement, the RF power P_{RF} must be reduced to approximately 500 mW. Next, the RF frequency f_{RF} of the AOM is varied around its design value, and again, the power of the 1st order and the distance between the 0th and 1st orders are recorded. We remain within a range of 60 MHz-100 MHz and choose a step size of a few MHz. Subsequently, we compare the frequency dependence of ϵ obtained from the measurement as well as the Bragg angle θ_B with theory and experimentally determine the quality factor Q through an appropriate fit.

3.2.4 Measurement of angular dependence and comparison of the quality factor

Now, the AOM is operated again at its central RF frequency f_0 (80MHz). The angle of the AOM is adjusted around its optimal value within a range of $\pm 1^\circ$, and once again, we record the power of the 1st order. A sensible step size was chosen again, which also varies a bit, to obtain more data in regions of greater change. Here too, the measurement is compared with theory, and we verify whether the quality factor in this measurement matches that from the previous measurement.

3.2.5 Measurement of the angular dependence of the maximum diffraction efficiency

Prior to the measurement, the RF power P_{RF} must be reduced to approximately 500mW. Next, the RF frequency f_{RF} of the AOM is varied within the range of 60 MHz-100 MHz. However, this

time, the Bragg angle is adjusted and optimized for each frequency. Once again, the power of the 1st order is recorded.

4 Ergebnisse

This section discusses the found results of our experiment, including the calculation of the following characteristics of the AOM: the Bragg angle, the saturation power, two different quality factors, and the speed of sound inside the crystal.

4.1 Measurement of the Bragg angle

After finding the angle where the power of the 1st order is maximized, to find the optimal angle, we measured a distance of $d = 2,0(1)$ cm. The error is related to the minimal distance of 1 mm on the ruler and how accurately we can find the centerpoints of the light. From this distance, we obtained a Bragg angle of $\theta_B = 6,0(3)$ mrad, which is consistent with the value given by the manufacturer.

4.2 Measurement of intensity dependence and determination of saturation power.

Next, we measured the outgoing and incoming power of the laser to calculate the insertion loss. This gave $P_{\text{in}} = 906,9(1)$ μW with a background radiation of $P_{\text{in,back}} = 5,881(7)$ μW and $P_{\text{out}} = 858,3(3)$ μW with a background radiation of $P_{\text{out,back}} = 5,289(14)$ μW . All power measurements here and in the experiments to come are done by averaging over a time of around 20 s, taking the mean error and average value. After subtracting the background, we calculated an insertion loss of $IL = 0,0532(3)$. This is consistent with the producer's value of $IL = 0,05$. To find the saturation power of the AOM, we varied the peak-to-peak voltage from 0 mV to 600 mV, which had to be converted into the power of the RF-wave using Formula 9. Then, we measured the power of the 0th order and 1st order. At the point of measurement, we found a background light of $P_{\text{back}} = 7,43(26)$ μW , which was subtracted from all points. The collected data is shown in Figure 7. Here, we can plot a fit from the function 6 to calculate the saturation power. For the fit of the 0th order, we modified the function by shifting it 90° . From the fit function, we obtained a saturation power of $P_{\text{sat}} = 1,351(19)$ W for the 0th order and $P_{\text{sat}} = 1,291(17)$ W for the 1st order. This deviates from the saturation power $P_{\text{sat}} = 1$ W given by the manufacturer. This could be explained by a miscalibration of the experiment; for example, the amplification of the amplifier could differ from our estimated value. The calculated maximum and minimum efficiencies of $\epsilon_{1,\text{max}} = 0,935(6)$, $\epsilon_{0,\text{max}} = 0,967(18)$, and $\epsilon_{0,\text{min}} = 0,010(5)$ also deviate slightly from the efficiencies given by the producers of $\epsilon_{1,\text{max}} = 0,9$ and $\epsilon_{0,\text{max}} = 1$, which could be due to the previously mentioned error or some other power loss between the measurement point of the outgoing power and the power of the maxima.

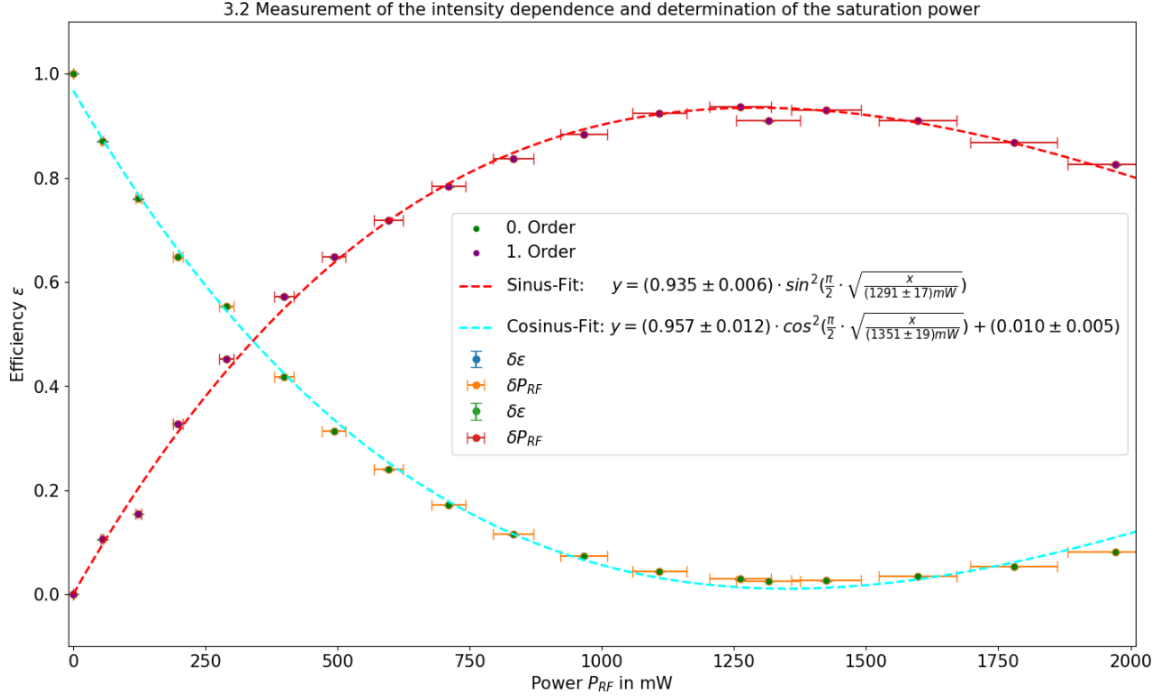


Figure 7: The diagram depicts the efficiency ϵ of the 0th and 1st orders plotted against the radio-frequency power P_{RF} . The green data points represent the 0th order, and a cosine fit: $y = (0,957 \pm 0,012) \cdot \cos^2(\frac{\pi}{2} \cdot \sqrt{\frac{x}{(1351 \pm 19)\text{mW}}}) + (0,010 \pm 0,005)$ has been applied. The purple data points represent the 1st order, and a sine fit: $y = (0,935 \pm 0,006) \cdot \cos^2(\frac{\pi}{2} \cdot \sqrt{\frac{x}{(1291 \pm 17)\text{mW}}})$ has been applied.

4.3 Measurement of frequency dependence and determination of the quality factor

After decreasing the power of the RF back to 500 mW, we then varied the RF frequency from 60 MHz to 100 MHz around its center frequency to find the relation of the efficiency to the frequency of the wave. From the resulting curve shown in Figure 8, we can calculate the quality factor given by equation 8. The resulting curve does not fit our data very well. The curve has its maximum at the center frequency $f_0 = 80$ MHz. It is clear to see that the maximum of the curve and the maximum in our data don't overlap. This led us to the conclusion that the center frequency of our AOM does not align with the one given by the manufacturer. So, we included the center frequency as a variable to fit. This gave a much better fit, as shown in Figure 9. From the fit function, we obtained a new center frequency of $f_{0,\text{new}} = 85,6(3)$ MHz and a quality factor of $Q = 0,622(5)$. A reason that the center frequency should change could be the AOM degrading over its use time, which could change some of its properties, or again that the power of the amplifier shifted during the experiment.

We also measured the distance between the 0th and 1st orders to calculate the change of the angle. This could be used to calculate the sound velocity inside the crystal of the AOM by using Equation 3 and the Bragg condition Equation 1. From that, we find that the Bragg angle should change linearly with the frequency. This is shown in Figure 10. From this, we calculated that the speed of sound should be $V_s = 4,7(2)$ km/s. This measurement is not perfectly accurate

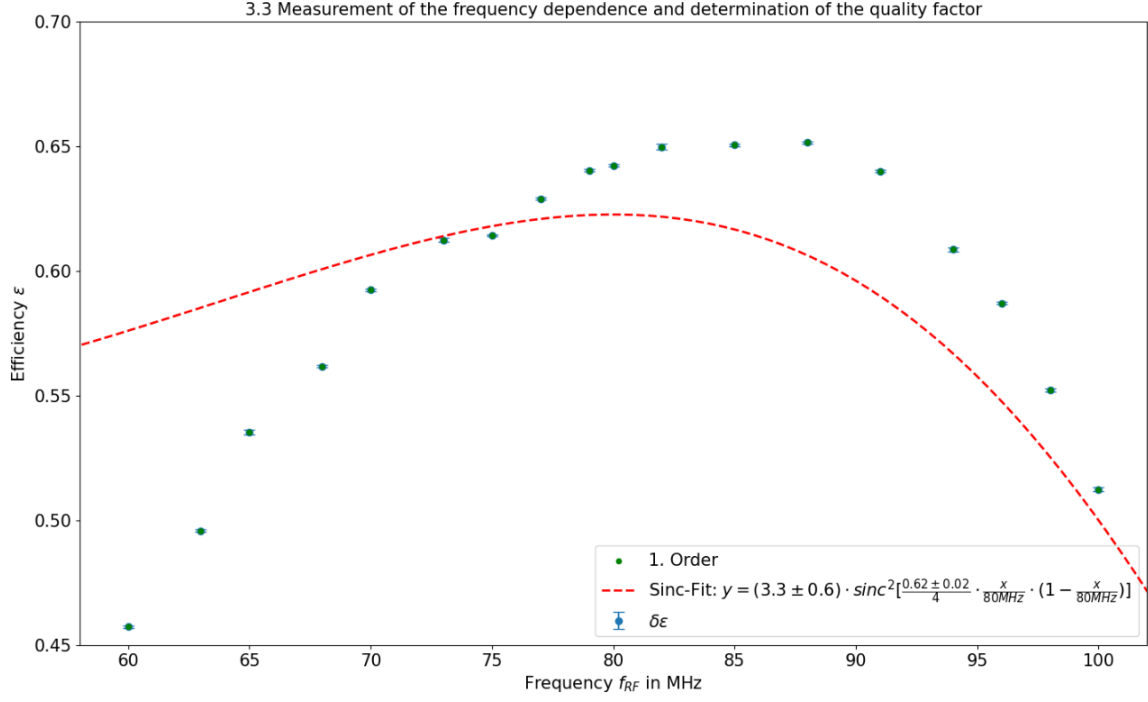


Figure 8: The diagram illustrates the efficiency ϵ of the 1st order plotted against the radio-frequency frequency f_{RF} . A sinc fit has been applied, described by the equation $y = (3,3 \pm 0,6) \cdot \text{sinc}^2\left[\frac{0,62 \pm 0,02}{4} \cdot \frac{x}{80\text{MHz}} \cdot \left(1 - \frac{x}{80\text{MHz}}\right)\right]$.

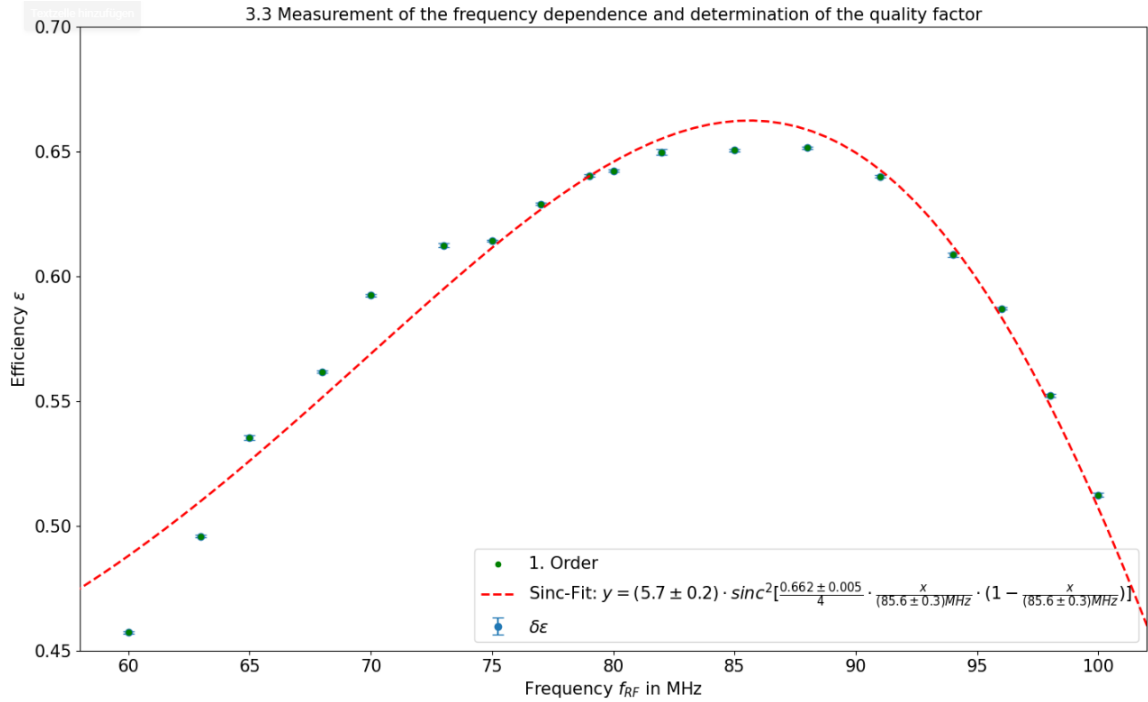


Figure 9: The diagram illustrates the efficiency ϵ of the 1st order plotted against the radio-frequency frequency f_{RF} . A sinc fit has been applied, described by the equation $y = (5,7 \pm 0,2) \cdot \text{sinc}^2\left[\frac{0,622 \pm 0,005}{4} \cdot \frac{x}{(85,6 \pm 0,3)\text{MHz}} \cdot \left(1 - \frac{x}{(85,6 \pm 0,3)\text{MHz}}\right)\right]$. In this case, additionally, the center frequency was also chosen as a fitting variable to improve the fit.

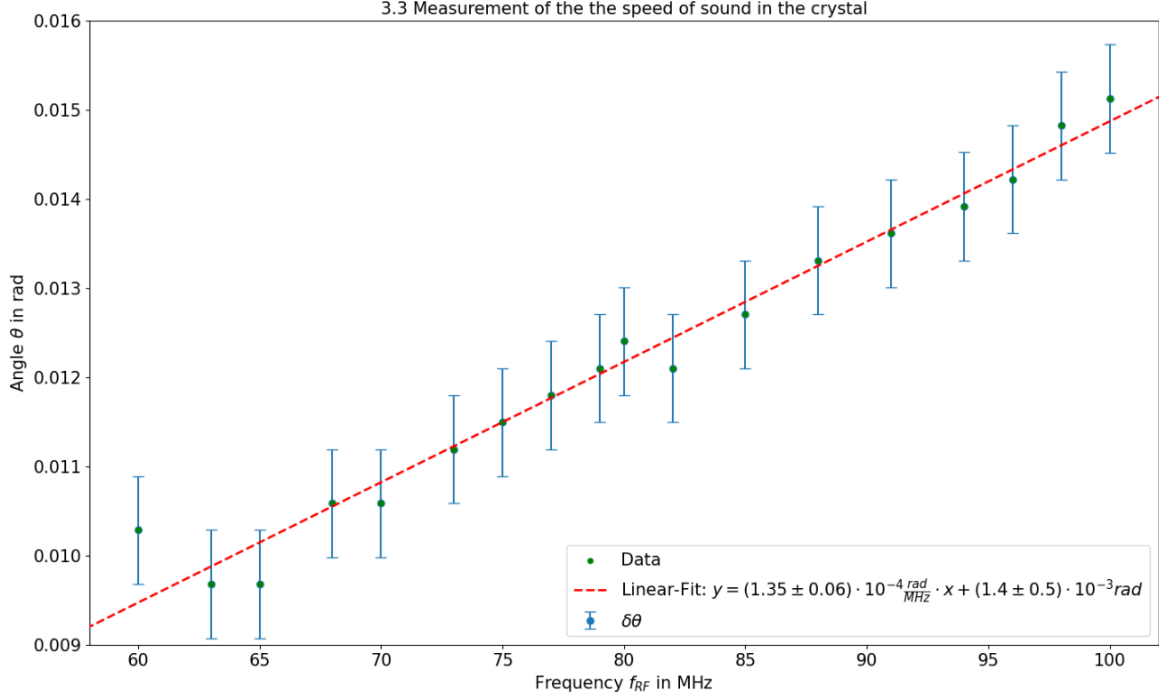


Figure 10: The diagram depicts the angle θ between the maxima of the 0th and 1st orders plotted against the radio-frequency frequency f_{RF} . A linear fit with the function $y = (1,35 \pm 0,06) \cdot 10^{-4} \frac{\text{rad}}{\text{MHz}} \cdot x + (1,4 \pm 0,5) \cdot 10^{-3} \text{rad}$ has been applied.

because we did not change the angle of the AOM perfectly into the maximum intensity, leading to a slight change of the angle.

4.4 Measurement of angular dependence and comparison of the quality factor

After putting the RF back to a frequency of 80 MHz, we now change the angle of the crystal. For that, we turn the crystal with a screw. This screw turns the AOM for 1° for one revolution. The screw has 25 markings on it which are evenly spaced; we were able to adjust the screw down to one quarter of one marking, giving us the uncertainty for the angle. We took measurements around 1° of the Bragg angle and recorded the power at that point. In Figure 11, the resulting data is shown. From Equation 7, we can fit the data to calculate the quality factor.

The resulting fit overlaps with the data very well, and we find a quality factor of $Q = 0,645(7)$. This does not perfectly align with the one measured in Section 4.3 but is very close to that value. This deviation is not that surprising, having done two different experiments where outside factors could have slightly changed. In the end, we are confident in saying that the quality factor of the AOM at a power of 0,5 W is 0,63(2).

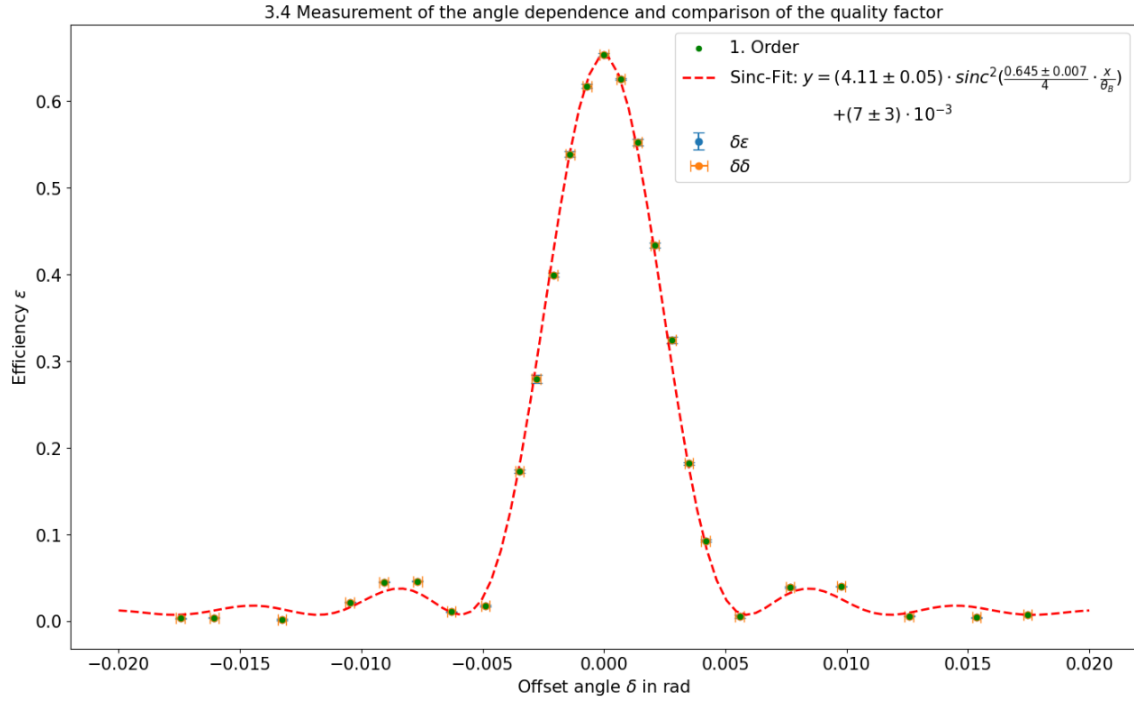


Figure 11: The diagram illustrates the efficiency ϵ of the 1st order plotted against the offset angle δ . A sinc fit with the function $y = (4,11 \pm 0,05) \cdot \text{sinc}^2\left(\frac{0,645 \pm 0,007}{4} \cdot \frac{x}{\theta_B}\right) + (7 \pm 3) \cdot 10^{-3}$ has been applied.

4.5 Measurement of the angular dependence of the maximum diffraction efficiency

Lastly, we measured the power dependent on the frequency again, but this time we adjusted the AOM to maximize the power. The resulting data is shown in Figure 12.

Again, we see that the peak efficiency is not at the center frequency of 80 MHz; instead, we observe a shift to around 85 MHz. This supports the theory that the power gain through the amplifier was wrongly estimated.

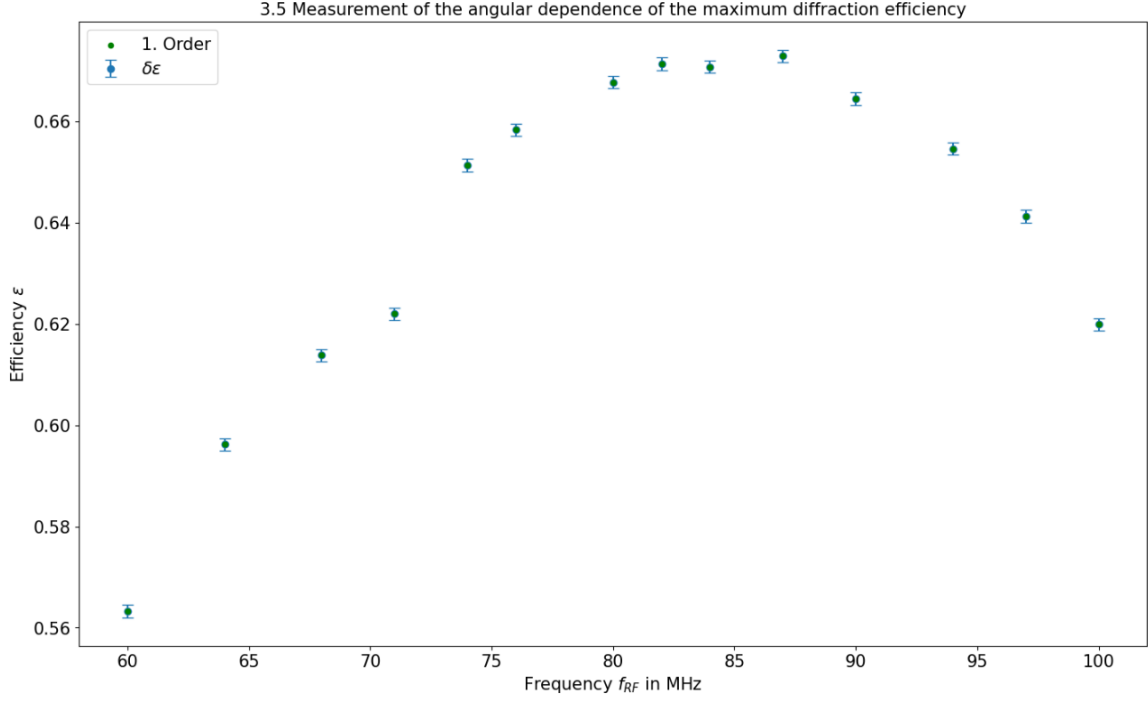


Figure 12: The diagram illustrates the efficiency ϵ of the 1st order plotted against the radio-frequency frequency f_{RF} .

5 Disscution

In this experiment, we were able to characterize the AOMO 3080-125 by measuring the efficiency of the 0th and 1st orders. By varying the power of the RF, we calculated a saturation power of 1320(30), deviating from the value provided by the producer. We also demonstrated that the efficiency change is consistent with the one given by the producer. Next, we varied the RF frequency, and from this, we could show that the central frequency is 85,6(3) MHz and that the AOM has a quality factor of 0,622(5). This was confirmed by de-aligning the angle of the AOM, from which measurement we found the quality factor to be 0,645(3), which is consistent with the first one. Lastly, we were able to calculate the speed of sound inside the crystal of the AOM to be 4,7(2) km/s. With all this data, we characterized the AOM.

References


- [1] U. Innsbruck. *Fortgeschrittenenpraktikum Versuch 08: Akusto-optischer Effekt*. Skript; Status: 7. February 2024. Retrieved on 22. April, 2024.
- [2] Wikipedia. *Acousto-optic modulator*. Online; Stand 4. December 2023. Retrieved on 22. April 2024. 2023. URL: https://en.wikipedia.org/wiki/Acousto-optic_modulator.
- [3] LEIFIphysik. *BRAGG-Reflexion*. Online; Retrieved on 22. April 2024. 2024. URL: <https://www.leifiphysik.de/optik/beugung-und-interferenz/grundwissen/bragg-reflexion>.
- [4] T. starter rashida564. *Electron Gun diffraction and undeflected spot diameter*. Online; status 8. March 2019. Retrieved on 22. April 2024. 2019. URL: <https://www.physicsforums.com/threads/electron-gun-diffraction-and-undeflected-spot-diameter.968354/>.
- [5] E. A. *Acousto-optical modulators (AOM)*. Online; status 3. November 2019. Retrieved on 23. April 2024. URL: <https://elent-a.net/acousto-optic-modulators-aom/>.

Explanation

Hereby, we confirm that the present report has been independently authored and that all necessary sources and references have been provided.

Arik Bürkle	23.04.2024
Student 1	Date

Robin Hoffmann	23.04.2024
Student 2	Date

	
Valentin Ertl	23.04.2024
Student 3	Date